Void thermalization response of a self-powered neutron detector

by

Ronald Lionel Harris

A Thesis Submitted to the
Graduate Faculty in Partial Fulfillment of
The Requirements for the Degree of
MASTER OF SCIENCE

Department: Chemical Engineering and Nuclear Engineering
Major: Nuclear Engineering

Iowa State University
Ames, Iowa

1976

TABLE OF CONTENTS

LIST OF FIGURES

LIST OF TABLES

I. INTRODUCTION

The field of reactor noise has received considerable interest recently because the noise output of a reactor contains a good deal of information about the reactor system. It is hoped that this information can provide an early warning of anomalous behavior or malfunction of reactor components. However, much more theoretical knowledge is needed about the processes which cause reactor noise before a practical and reliable anomaly detection system can be devised.

One of the important sources of noise in a Boiling Water Reactor (BWR) is the moderator void fraction fluctuations which occur throughout most of the core because of the random characteristics of the boiling process. Since these void fraction fluctuations vary the properties of the moderator, the neutron flux is affected. These effects on the neutron flux can be measured by means of a neutron detector and are termed neutron noise. There are many other mechanisms which also cause neutron noise, but some authors [1;2] believe that the predominant noise source in a BWR is the void fraction fluctuation.

Self-powered neutron detectors have been used extensively in studying reactor noise [3;4;5] because their small size and ruggedness allows them to be placed virtually anywhere in a reactor core. In view of the fact that void fraction

fluctuations are an important noise source and that self-powered neutron detectors are used in studying noise, a study isolating the effects of void fraction on the output of a self-powered neutron detector is needed.

The approach of this study is to model on a computer the situation in which a self-powered neutron detector is placed in a BWR fuel bundle. The void fraction fluctuations are represented by varying the void fraction of the moderator near the detector while holding the void fraction of non-local moderator constant at a realistic average in order to study the effect of local void fraction fluctuations on the detector.

The computer codes used in this study include LEOPARD, which provides the neutron cross section data needed by FOG, which calculates neutron fluxes usable in SPOND, which in turn computes the detector current output for the void fraction of interest. A series of void fraction values is processed in this manner to provide a composite picture of the dependence of the detector output on void fraction. The calculation is repeated for a prompt-response self-powered neutron detector using two different emitter materials. Since the emitter materials are sensitive mostly to thermal neutrons, the detector current outputs are expected to be strongly dependent on the thermal flux changes due to void fraction variations.

II. LITERATURE REVIEW

The effect of the void fraction on the signal developed by a neutron detector has been studied by several authors such as Rothmann [2], Wach and Kosaly [6], and Kosaly et al. [7] by means of random data analysis techniques. Unfortunately, these works seem to center primarily on the cases of bubbly flow or plug-slug flow (See Figure 2.1) in which the void fraction is fairly low when, in fact, the annular flow regime is of most interest in the boiling water reactor in which the void fraction can be considerably higher [8].

This work uses a different approach in that it ignores

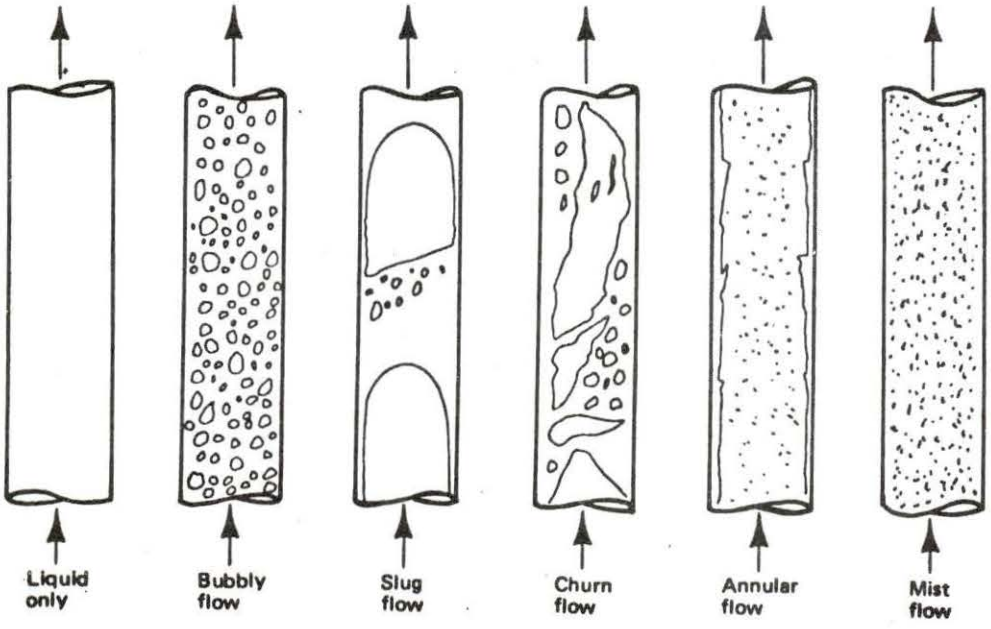

Figure 2.1. Typical flow regime patterns in vertical flow

the statistics of the void fraction fluctuations, on which no widespread agreement has been reached, and investigates the current output of a self-powered neutron detector as a function of void fraction by means of a series of steady-state steps. A wide range of void fractions is studied by a fairly accurate computer model of the actual situation of interest, the core of a boiling water reactor.

III. THE SELF-POWERED NEUTRON DETECTOR

A. General Description

The distinguishing feature of the self-powered neutron detector is that it requires no external voltage supply. Self-powered neutron detectors have small physical dimensions, a relatively high reliability, a low burnup rate, an operating range extending up to more than 570 °F, and a moderate price. Because of these characteristics and the fact that it is solid state and therefore quite rugged, it is particularly suited for in-core measurements.

A self-powered neutron detector consists of three main parts as shown in Figure 3.1. They are: a wire-shaped emitter; a ceramic insulator; and a sheath-like metallic collector. These components are generally arranged in a coaxial geometry. Emitter length may vary from 10-20 cm; diameter, from 0.05 to 0.20. The outer diameter of the collector is usually 0.15-0.40 cm. The insulator is typically Al_2O_3 with a thickness of 0.05 cm.

There are two main types of self-powered neutron detectors, the prompt-response and the delayed-response versions, with the emitter material determining the type. Emitter materials such as Cobalt, Cadmium, Erbium, and Hafnium are used in prompt detectors, while Vanadium and Rhodium are used in delayed-response detectors. Current in a prompt-response detector is produced predominantly by Compton electrons re-

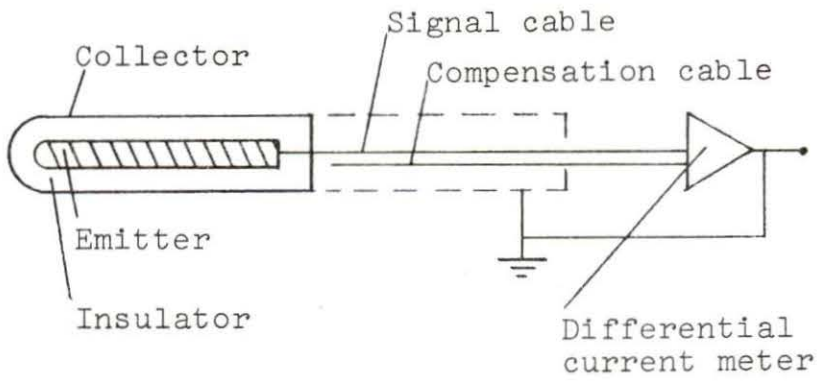

Figure 3.1. Configuration and measuring arrangement of a self-powered neutron detector

leased after self-absorption of the neutron capture gamma-ray cascade by the emitter, while current in a delayed-response detector is produced predominantly by beta particles emitted by neutron activation products. In both cases the negatively charged particles (electrons or beta particles) leave the emitter and cross the insulator to the sheath, resulting in a positively charged emitter. Delayed and prompt effects are present in both types of detectors, but emitter material determines which effect will predominate. Beta particles emitted from decay of Co-60 create unwanted background noise. Conversely, in delayed-response detectors current produced by the prompt effect constitutes a background noise. Response time of delayed-response detectors is determined by decay time of radioisotopes in the emitter. In the case of the Rhodium emitter the radioisotope is Rh-104 with a half-life of 42 seconds, whereas in the Vanadium emitter the radioisotope

is V-52 with a half-life of 3.76 minutes.

Since this thesis is concerned with the detector response to local void fraction fluctuations the prompt-response detector is of greater interest because its current output more nearly follows neutron flux fluctuations.

B. Mathematical Model for Prompt-Response Self-Powered Neutron Detectors

Jaschik and Seifritz have developed a sophisticated model for calculating the prompt-response of a self-powered neutron detector [3]. The model yields an expression for current output in amps per centimeter of emitter length per unit flux. The following parameters are taken into account in the model:

1) Neutron self-shielding of the emitter

2) Flux depression correction

3) Compton and photoelectron production rate due to self-absorption by the emitter of the gamma-ray cascade emitted immediately after neutron capture

4) Electron escape probability from the emitter

5) Loss of electron energy within the emitter

6) Range of the electrons in the insulator which contains a space-charge electric field.

A schematic representation of the prompt-response self-powered neutron detector model is given in Figure 3.2.

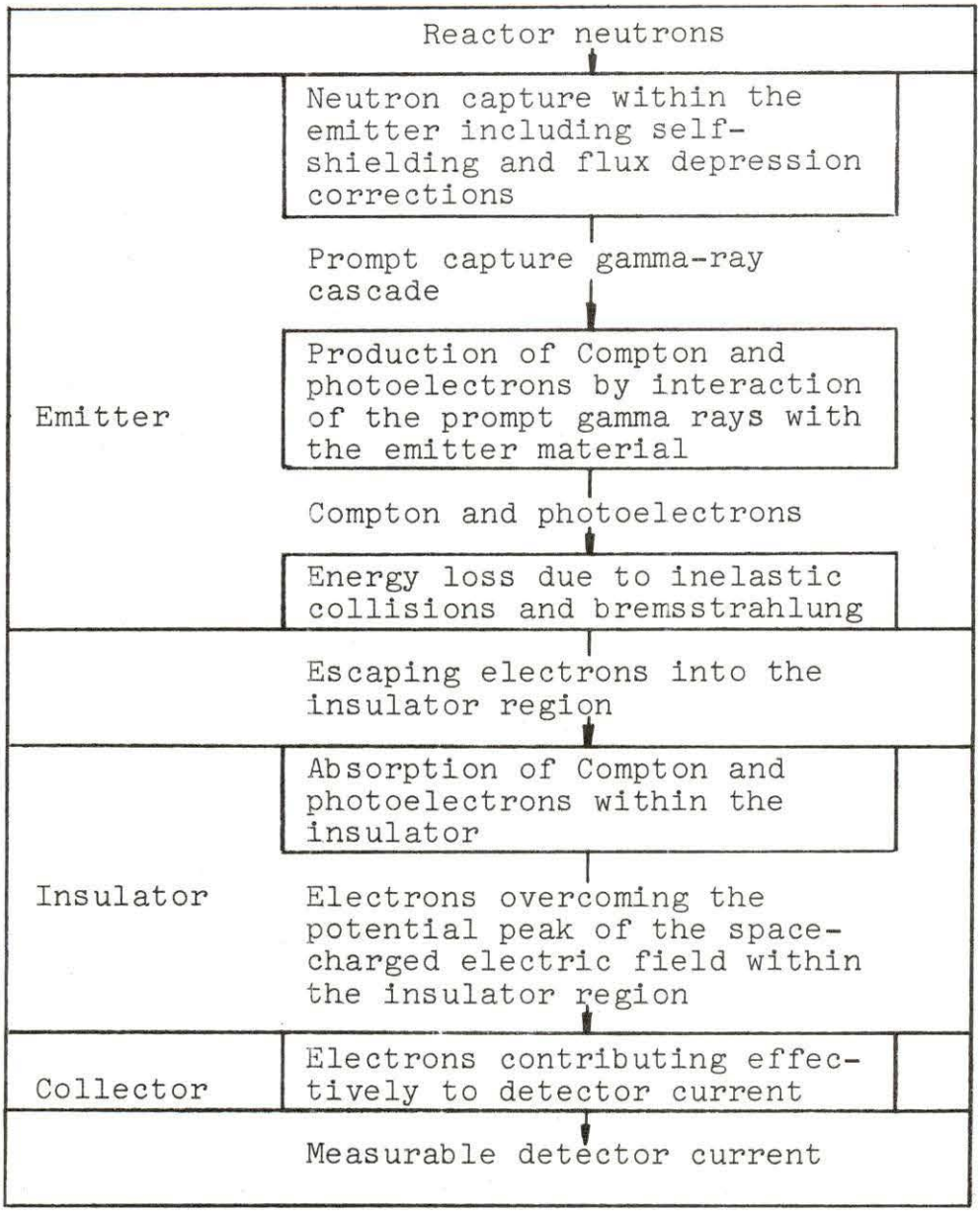

Figure 3.2. Mathematical model schematic of prompt-response self-powered neutron detector

The basic equation given by the Jaschik-Seifritz model is:

$$I_e = e \times \left[(V/L)\int_0^{E_n,max} \Sigma(E_n)\cdot\Phi(E_n)\cdot f(E_n)\cdot F(E_n)\,dE_n\right]$$

$$\times \left[\sum_{i=1}^{2}\int_0^{E_\gamma,max} \varepsilon_i(E_\gamma)\cdot P_i(E_\gamma)\cdot Y(E_\gamma)\,dE_\gamma\right] \qquad (3.1)$$

where

I_e = unit detector current in amps per centimeter of emitter length

e = electronic charge, 1.602×10^{-19} amp-sec per electron

V = emitter volume, cm^3

L = emitter length, cm

E_n = incident neutron energy

E_n,max = maximum neutron energy

$\Sigma(E_n)$ = macroscopic neutron capture cross section of the emitter material at neutron energy E_n, cm^{-1}

$\Phi(E_n)$ = differential neutron flux at neutron energy E_n, neutrons/cm^2-sec-unit energy

$f(E_n)$ = neutron self-shielding factor of the emitter at neutron energy E_n

$F(E_n)$ = flux depression factor of the emitter at neutron energy E_n

$\varepsilon_i(E_\gamma)$ = electron escape efficiency, i. e., probability of a Compton (i=1) or a photo-electron (i=2) produced within the emitter by a prompt capture gamma ray with energy E_γ,

leaking out of the emitter, crossing the insulator, and reaching the collector

$P_i(E_\gamma)$ = first-collision probability of prompt capture gamma rays in the emitter, i. e., the probability of the production of an electron by Compton (i=1) or photon (i=2) interaction of a gamma ray with energy E_γ

$Y(E_\gamma)$ = yield of capture gamma rays, i. e., the number of gamma rays per gamma interval per neutron captured in the emitter.

The first bracketed term gives the neutron capture rate per unit emitter length. The second term in brackets represents the probability that the capture of a neutron effectively contributes to the detector current output.

For a more detailed discussion of the model and an explanation of how the values are obtained for each of the terms the reader is referred to the original article [3].

The model yielded results (Ref. [3]) with an accuracy of ±12% in the most unfavorable case when compared to actual experimental data obtained from several self-powered neutron detectors placed in a reactor. For the two emitter materials used in this work the calculated results were within ±10% of the measured results.

IV. DESCRIPTION OF LOCAL VOID FRACTION MODEL

Since it is the aim of this work to obtain information about the effects of voids on the output of a self-powered neutron detector placed in a Boiling Water Reactor (BWR), that situation must be accurately modeled. In the previous section a mathematical model was outlined to determine the detector output for a given neutron flux. A local void fraction model (See Figure 4.1) must characterize the neutron flux in a BWR and account for the manner in which it is modified by the presence of voids. Basically this has been done by representing the BWR fuel bundle under operating conditions by a unit cell environment consisting of a single fuel rod surrounded by a local moderator region within a homogeneous mixture of fuel, cladding, and moderator. A self-powered neutron detector has been substituted for the fuel in the rod. The void fraction in the unit cell is varied to represent local void fluctuations in the moderator. Multi-group diffusion theory is used to determine the neutron flux in energy and magnitude at the location of the detector emitter. Using the calculated neutron flux the Jaschik-Seifritz model can be used to find the detector output.

The Duane Arnold Energy Center (DAEC) BWR at Palo, Iowa, is taken as a representative boiling water reactor. Numerical data has been collected by Paustian [9] in an investigation which considers the Palo reactor. The data is summarized in

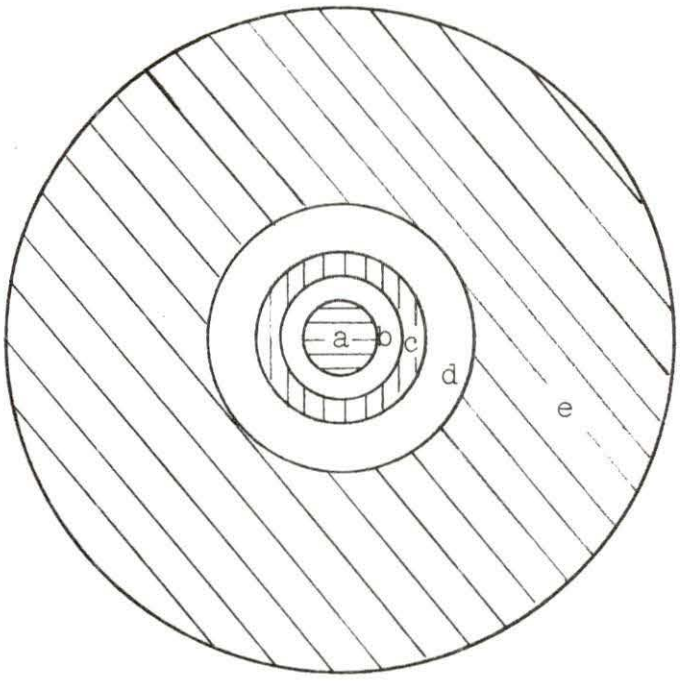

Region	Material	Region Thickness
a	Al_2O_3 Insulator	0.150 cm
b	Nickel Sheath	0.472 cm
c	Zircaloy-2 Cladding	0.094 cm
d	Moderator (H_2O)	0.346 cm
e	Homogeneous Fuel Bundle	6.375 cm

Figure 4.1. Local void fraction model

Table 4.1. A DAEC BWR unit cell is shown in Figure 4.2.

A sketch showing the geometry of the local void fraction model is given in Figure 4.1. The volume occupied by the model is equivalent to that of a fuel bundle found in the DAEC BWR, and the unit cell containing the detector occupies

Table 4.1. Pertinent DAEC BWR data

Thermal and Hydraulic Design	
Reference design thermal output, Mw(th)	1593
System pressure, psia	1020
Average power density, kw/liter	51.0
Average thermal output, kw/ft	7.067
Core maximum exit voids within assemblies, %	76
Core average exit quality, % steam	14.3
Fuel Design	
Fuel rod array	7 x 7
Fuel rod outside diameter, inch	0.563
Fuel rod clad thickness, inch	0.037
Gap-pellet to clad, inch	0.006
Clad material	Zircaloy-2
Fuel pellet material	UO_2
Pellet density, % theoretical	93
Pellet diameter, inch	0.477
Pellet length, inch	0.5
Fuel rod pitch, inch	0.738
Space between fuel rods, inch	0.175
Number of fuel assemblies	368
Number of fuel rods per assembly	49
Overall length of fuel assembly, inches	175.88

Table 4.1. (Continued)

Core Assembly	
Equivalent core diameter, inches	129.9
Core height (active fuel), inches	144

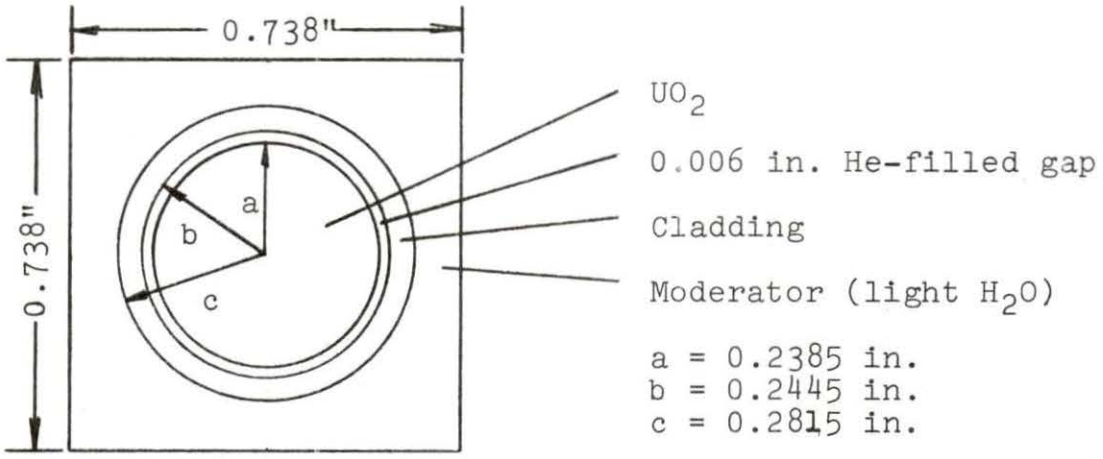

Figure 4.2. DAEC BWR unit cell

a volume equivalent to that of a unit cell in the DAEC BWR. An enlarged cross section view of the detector is found in Figure 4.3. All dimensions are corrected for operating temperatures at a position about halfway up the reactor core corresponding to an average moderator void fraction of 0.50 as calculated by Paustian [9].

As was previously mentioned, the bulk of the model is made up of an homogenized BWR fuel bundle so that it can be

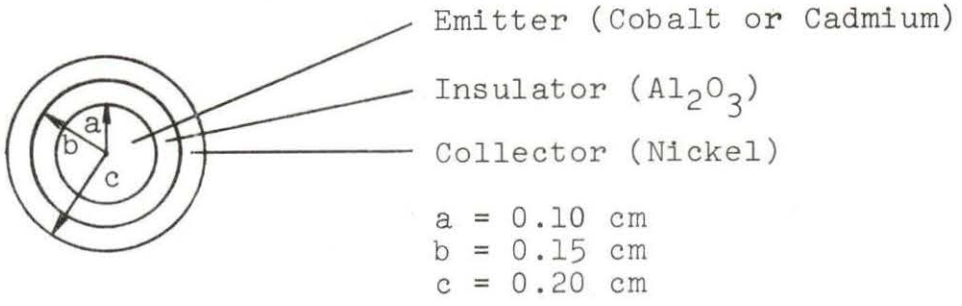

Figure 4.3. Cross section of self-powered neutron detector

considered as a single phase region made up of an evenly dispersed mixture of all atoms found in the actual fuel bundle, including fuel, cladding, and moderator (void fraction, 0.50). This permits one-dimensional calculations, requiring less time and effort. For the same reasons the local moderator region is also considered homogeneous although in actuality it is a two-phase mixture. As the void fraction is varied in the calculations the relative number of molecules in that region is varied accordingly. The Nickel detector sheath is also considered homogeneous, filling the gap between the detector sheath and the cladding tube.

Reactor flux is calculated using diffusion theory since there are no strong sources or absorbers, and nuclear properties in the various regions are reasonably uniform. Calculations reveal that the flux is slowly varying. Isotropic scattering is assumed for simplicity because comparative results are all that are sought.

Boundary conditions assumed for solution of diffusion

equations are that derivatives of the flux with respect to position are equal to zero at both the center of the detector and at the outer boundary of the homogenized fuel bundle.

To maintain a constant total reactor power a normalization of fluxes was made to compensate for variations due to local void fraction effects.

V. COMPUTER PROGRAMS AND CALCULATION PROCEDURES

A. Introduction

Three computer programs are used sequentially in performing the calculations in this study. The first program used is LEOPARD which produces few group cross sections for materials found in a nuclear reactor unit cell given such information as unit cell composition, temperatures, moderator void fraction and pressure, dimensions, and geometry. Secondly, the computer code, FOG, using the material cross sections found by LEOPARD, is utilized to give the neutron flux distribution in the void fraction model so that the flux at the self-powered neutron detector emitter can be determined. And finally, a computer code, SPOND, developed by the author, which is based on the detector model proposed by Jaschik and Seifritz [3], calculates the detector output given the neutron flux at the emitter.

Hand calculations include changing the local material microscopic cross sections found by LEOPARD into macroscopic cross sections usable by FOG and normalizing the FOG neutron flux data which is then used for input into the detector computer code.

LEOPARD and FOG were used in this study because they were readily available, inexpensive, and well documented as a consequence of extensive use here at Iowa State University.

B. The LEOPARD Code

LEOPARD, an acronym for Lifetime Evaluation Operations Pertinent to the Analysis of Reactor Design, computes temperature corrected microscopic cross sections for all materials specified as present in a reactor unit cell and macroscopic cross sections for a hypothetical homogeneous reactor unit cell containing those same materials in the same specified quantities. The code has the capability of handling up to four neutron energy groups, and also contains an option which calculates fuel depletion effects in discrete burnup steps for a dimensionless reactor. In this study, however, LEOPARD was used only to calculate cross sections, neglecting fuel depletion effects.

The LEOPARD program assumes a unit cell configuration consisting of three primary regions: fuel, cladding, and moderator-coolant. A fourth fictitious "extra" region, which can be optionally specified, may be used to take into account structural members, water slots, fuel assembly walls, control rods, etc., which may occupy a significant fraction of the total reactor core even though these materials are not present in a unit cell. The program can be used to treat either cylindrical or plate-type fuel elements. Lattice geometry, typically square or hexagonal, and buckling must be specified.

The composition of the reactor unit cell of interest is

read into the code by referring to the index number of a given material according to LEOPARD's library of materials and then giving the volume fraction of that material for each region. Moderator voids or a pellet-to-cladding gap may be represented by calculating the over-all volume fraction of the moderator ar cladding material assuming the region includes the void or gap. That is, the void or gap is represented by homogenization. In this manner any moderator void fraction that is desired can be represented. Elements for which it is not possible to determine the volume fraction, such as U-235, can be entered as "trace elements", and the weight fraction or atom fraction is given instead.

The temperatures for each region, dimensions of the unit cell, fuel pellet density, and reactor pressure are required so that LEOPARD can compute the correct atom densities and cross sectional data for operating pressures and temperatures.

For detailed information explaining the use of LEOPARD the reader is referred to Barry [10]. A discussion of the neutron physics and approximations involved in the program are given in a companion report by Strawbridge [11] and Crudele [12].

C. The FOG Code

FOG can calculate one-dimensional diffusion theory flux profiles for up to 239 mesh points in as many as 40 different

spatial regions utilizing up to four neutron groups in planar, cylindrical, or spherical geometry. Other options of no particular interest in this work are available.

Input data for FOG mainly consists of the various macroscopic cross sections and diffusion coefficients, which may be entered by region or material, the dimensions of the regions, the buckling, and group fission spectrum integrals. Further details concerning the techniques used by FOG in solving the diffusion equations and the use of the code are available in a report by H. P. Flatt [13]. A comprehensive study of the finite difference approximations to derivatives and the treatment of boundary conditions by FOG has been carried out by Munson [14].

D. The SPOND Code

SPOND is a simple computer program which calculates the current output of a prompt-response self-powered neutron detector given the neutron flux at the detector emitter. It is based on the Jaschik-Seifritz model. The code has been set up to use four neutron energy groups, but it can easily be modified to handle as many as desired.

Required data includes the neutron energy group fluxes, the number of neutron energy groups, the detector emitter volume, radius, and length, the emitter neutron energy group-

averaged macroscopic absorption cross sections, data on electron escape efficiency, probability of electron production, yield of capture gamma rays for a given emitter material, and the number of gamma ray energy intervals used. Because the program was developed specifically for this study, the void fractions, the number of void fraction cases being run at one time, and the neutron and gamma ray energy group intervals are also required. However, most of this data is not actually used in the calculations.

A listing and flow chart of SPOND can be found in the Appendix.

E. Calculation Procedure Details

The calculation procedure consisted of making two LEOPARD runs to obtain cross section data for the DAEC unit cell and the modified DAEC unit cell containing the detector, 15 FOG runs corresponding to the various void fractions used, and 15 SPOND runs to obtain the detector current output for each void fraction case.

Two different LEOPARD calculations were carried out. One calculation determined the macroscopic cross sections for the DAEC BWR unit cell and thus directly furnished the information needed by FOG for the region consisting of the homogenized fuel bundle in the local void fraction model. The other calculation was similar but involved the addition of a

detector to the DAEC unit cell. This calculation was needed in order to obtain microscopic cross sections for the materials present in the inner regions of the local void fraction model, including the local moderator, cladding, and detector. The detector materials were entered into LEOPARD by making use of the "extra" region. Necessary data such as composition of the unit cell and operating temperatures and pressure was obtained from Paustian's thesis [9]. Some of the more important data may be found in Table 5.1. A detector position in the core corresponding to an average void fraction of 0.50 was chosen so that, presumably, void fraction fluctuations would be symmetrically distributed about the steady state value. Also, this position is quite close to being half-way up the reactor core and thus the detector is in the region of the maximum flux.

The LEOPARD output for the BWR unit cell with the detector present had to be converted from microscopic cross

Table 5.1. DAEC BWR unit cell data

Region	Volumetric Composition	Temperature (°F) at 6 ft. core height
Fuel	100% of UO_2	2220
Cladding	87.0% Zircaloy-2	605
Moderator	50% H_2O	547

sections to macroscopic cross sections for use in FOG by use of the following equation:

$$\Sigma = N \times \sigma \tag{5.1}$$

where

Σ = macroscopic cross section

N = atom density of material

σ = microscopic cross section of material.

In order to represent changes in void fraction the local moderator atom density was determined as follows:

$$N = N_o(1 - \alpha) \tag{5.2}$$

where

N = moderator atom density

N_o = moderator atom density for void fraction = 0

α = void fraction.

The cross section data for the various regions entered in FOG for a typical run (local moderator void fraction equal to 0.50) may be found in Table 5.2. FOG runs were made for void fraction values of 0.00, 0.10, 0.20, 0.30, 0.40, 0.50, 0.60, 0.70, 0.80, 0.90, 0.92, 0.94, 0.96, 0.98, and 0.99. A run was not made for a void fraction of 1.00 because of the difficulties which are presented in such a case to diffusion theory. Since isotropic scattering was assumed, the value of the diffusion coefficient was assumed to be given by the following equation:

$$D = 1/(3\Sigma_{tr}) \tag{5.3}$$

Table 5.2. Selected cross section data usable in FOG

Region	Material	Neutron group no.	Σ_s (cm^{-1})	$\nu\Sigma_f$ (cm^{-1})	Σ_a (cm^{-1})	Diff. Co. (cm)
a	Al_2O_3	1	0.01617	0.0	0.001234	3.831
		2	0.004387	0.0	0.00007887	1.805
		3	0.0008306	0.0	0.0005316	2.094
		4		0.0	0.002722	1.974
b	Ni	1	0.004124	0.0	0.0	31.00
		2	0.0004946	0.0	0.0	13.91
		3	0.0	0.0	0.0007233	4.360
		4		0.0	0.01063	3.867
c	Zr-2	1	0.02349	0.0	0.002508	2.181
		2	0.001064	0.0	0.0009157	1.044
		3	0.0	0.0	0.003768	1.212
		4		0.0	0.004087	0.9706
d	H_2O (0.50 void fraction)	1	0.04109	0.0	0.0003911	4.672
		2	0.05468	0.0	0.000004672	2.444
		3	0.05100	0.0	0.001760	1.904
		4		0.0	0.004365	0.6079
e	Homogeneous Reactor	1	0.04045	0.007729	0.004156	3.109
		2	0.03068	0.0005624	0.002316	1.505
		3	0.02264	0.007973	0.01906	1.215
		4		0.08839	0.05512	0.6508

where

D = diffusion coefficient

Σ_{tr} = macroscopic transport cross section.

Given this cross section data, FOG calculated the flux profile in four energy groups for the five regions using 15 intervals in region a, 9 intervals in region b, 9 intervals in region c, 15 intervals in region d, and 21 intervals in region e. Using this number of intervals gives a total of 70 mesh points used in the model calculations. The number of intervals was chosen to give a reasonable compromise between computational accuracy and economy. An individual calculation was needed for each void fraction case, so a total of 15 flux profiles were generated. Of primary interest, however, are the four-group flux values at the emitter location for the various void fraction cases. These values are provided in Table 5.3 along with the normalized source values at the outer boundary which were used in the normalization procedure. Table 5.4 furnishes the normalized flux values at the emitter location as computed by the following equation:

$$\Phi_n = (\Phi_i/\Phi_1) \times (S_1/S_i) \times 4.4 \times 10^{13} \qquad (5.4)$$

where

Φ_i = flux value to be normalized

Φ_1 = base case flux value (void fraction = 0)

Φ_n = normalized flux value

S_i = normalized fission source density calculated by

Table 5.3. Raw flux data at emitter surface

Void Fraction	Group 1	Group 2	Group 3	Group 4	Normalized Source
0.00	0.08154	0.1543	0.1173	0.05727	0.005799
0.10	0.08180	0.1551	0.1174	0.05621	0.005807
0.20	0.08205	0.1560	0.1175	0.05517	0.005814
0.30	0.08231	0.1568	0.1176	0.05418	0.005822
0.40	0.08256	0.1576	0.1177	0.05322	0.005829
0.50	0.08281	0.1584	0.1178	0.05229	0.005837
0.60	0.08305	0.1592	0.1180	0.05140	0.005845
0.70	0.08328	0.1600	0.1180	0.05053	0.005853
0.80	0.08350	0.1607	0.1181	0.04968	0.005861
0.90	0.08364	0.1613	0.1180	0.04882	0.005869
0.92	0.08364	0.1614	0.1179	0.04862	0.005871
0.94	0.08360	0.1613	0.1178	0.04840	0.005873
0.96	0.08348	0.1611	0.1174	0.04810	0.005875
0.98	0.08301	0.1600	0.1163	0.04752	0.005878
0.99	0.08203	0.1576	0.1142	0.04659	0.005882

FOG associated with the flux value to be normalized

S_1 = base case normalized source value at outer boundary.

The numerical value in Equation (5.4) is the average thermal flux in the reactor calculated from the average power density

Table 5.4. Normalized flux values at emitter surface

Void Fraction	Group[a] 1	Group[a] 2	Group[a] 3	Group[a] 4	Total[a] Flux
0.00	0.6264	1.185	0.9011	0.4400	3.153
0.10	0.6276	1.190	0.9007	0.4312	3.150
0.20	0.6287	1.195	0.9003	0.4227	3.147
0.30	0.6298	1.200	0.8999	0.4146	3.144
0.40	0.6310	1.205	0.8996	0.4068	3.142
0.50	0.6320	1.209	0.8991	0.3991	3.139
0.60	0.6330	1.213	0.8994	0.3918	3.137
0.70	0.6339	1.218	0.8982	0.3846	3.135
0.80	0.6347	1.221	0.8977	0.3776	3.131
0.90	0.6349	1.224	0.8957	0.3706	3.125
0.92	0.6347	1.225	0.8946	0.3689	3.123
0.94	0.6342	1.224	0.8936	0.3671	3.119
0.96	0.6330	1.222	0.8902	0.3647	3.110
0.98	0.6291	1.213	0.8815	0.3602	3.084
0.99	0.6213	1.194	0.8649	0.3529	3.033

[a]All fluxes divided by 10^{14}.

given for the DAEC reactor.

The normalized flux values were entered into the detector program, SPOND, which calculated the associated detector

current output. The procedure was repeated for each void fraction case. The emitter cross section data required by SPOND was obtained from a multi-group compilation provided by McElroy et al. [15]. The required four-group cross sections were obtained from the multi-group data by means of the following equation:

$$\bar{\sigma}_{i,j} = \left[\int_{E_j}^{E_{j+1}} \sigma_i(E)dE\right] \div \left[\int_{E_j}^{E_{j+1}} dE\right] \qquad (5.5)$$

where

σ = microscopic cross section

E = neutron energy.

The cross section data for the two emitter materials used in the SPOND program is summarized in Table 5.5. Additional data needed for the calculations was taken from the Jaschik-Seifritz paper [3].

Table 5.5. Cross section data for Cobalt and Cadmium

Neutron Group	Cobalt $\Sigma_a(cm^{-1})$	Cadmium $\Sigma_a(cm^{-1})$
1	0.00006476	0.2056
2	0.0004879	0.3271
3	0.09140	0.3150
4	1.3315	99.18

The effect of emitter material on detector output was explored by repeating the calculations for Cobalt and Cadmium. These two materials were chosen for consideration because they appear to be widely used in self-powered neutron detectors and because data for them was readily available. The results of these calculations are presented in the next section.

VI. RESULTS AND CONCLUSIONS

A. Results

The results of the calculations are given in tabular form in Table 6.1 and in graphical form in Figure 6.1 for both the Cobalt and Cadmium emitters. The detector response to a change in void fraction is virtually linear except for those cases in which the void fraction exceeds 0.90. If the detector current outputs are plotted versus thermal flux for the void fraction cases as in Figure 6.2 it can be seen that the detectors closely follow the thermal curve as expected.

That the detectors follow the thermal flux dependence

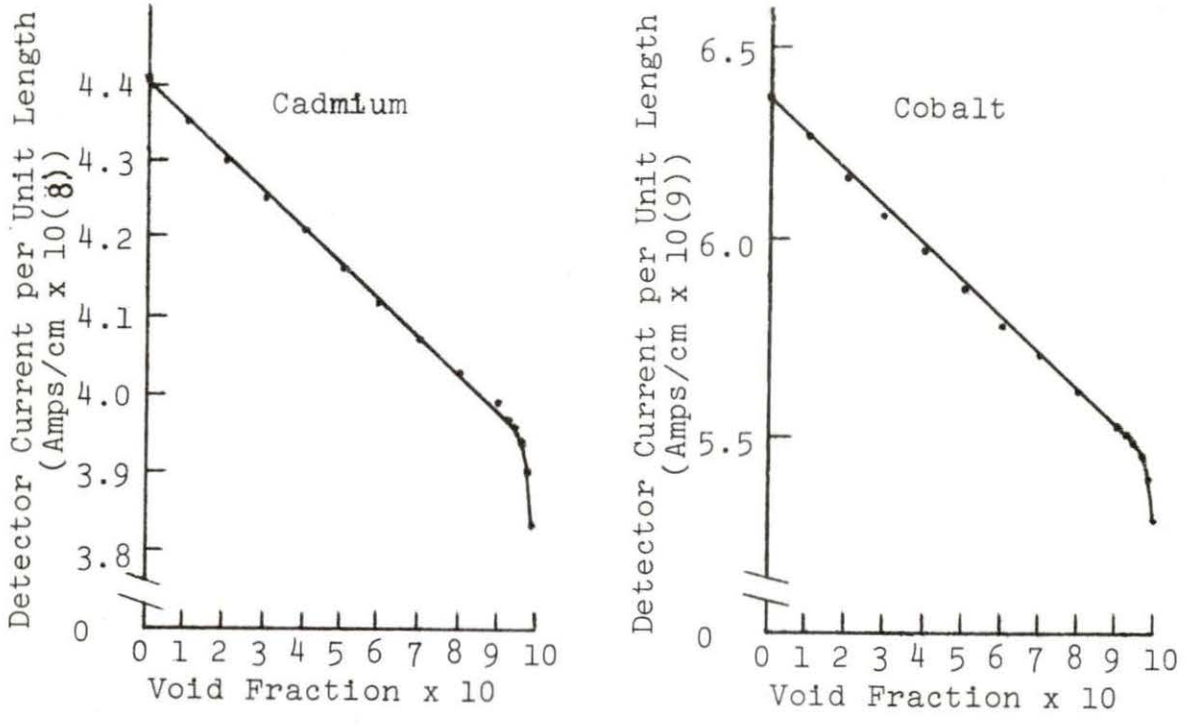

Figure 6.1. Current produced by self-powered neutron detectors for various void fractions

Table 6.1. Detector current output for various void fractions

Void Fraction	Cobalt Detector (Amps/cm x 10(9))	Cadmium Detector (Amps/cm x 10(8))
0.00	6.384	4.404
0.10	6.277	4.351
0.20	6.172	4.300
0.30	6.073	4.252
0.40	5.978	4.205
0.50	5.883	4.159
0.60	5.794	4.115
0.70	5.705	4.072
0.80	5.619	4.029
0.90	5.531	3.985
0.92	5.509	3.974
0.94	5.486	3.961
0.96	5.453	3.941
0.98	5.388	3.900
0.99	5.281	3.827

on void fraction is not surprising because upon close examination of the basic detector model equation (Equation (3.1)) it can be seen that the second term is a constant for a given emitter material. Thus, the only change in current output for a given detector is due to the change in the neutron

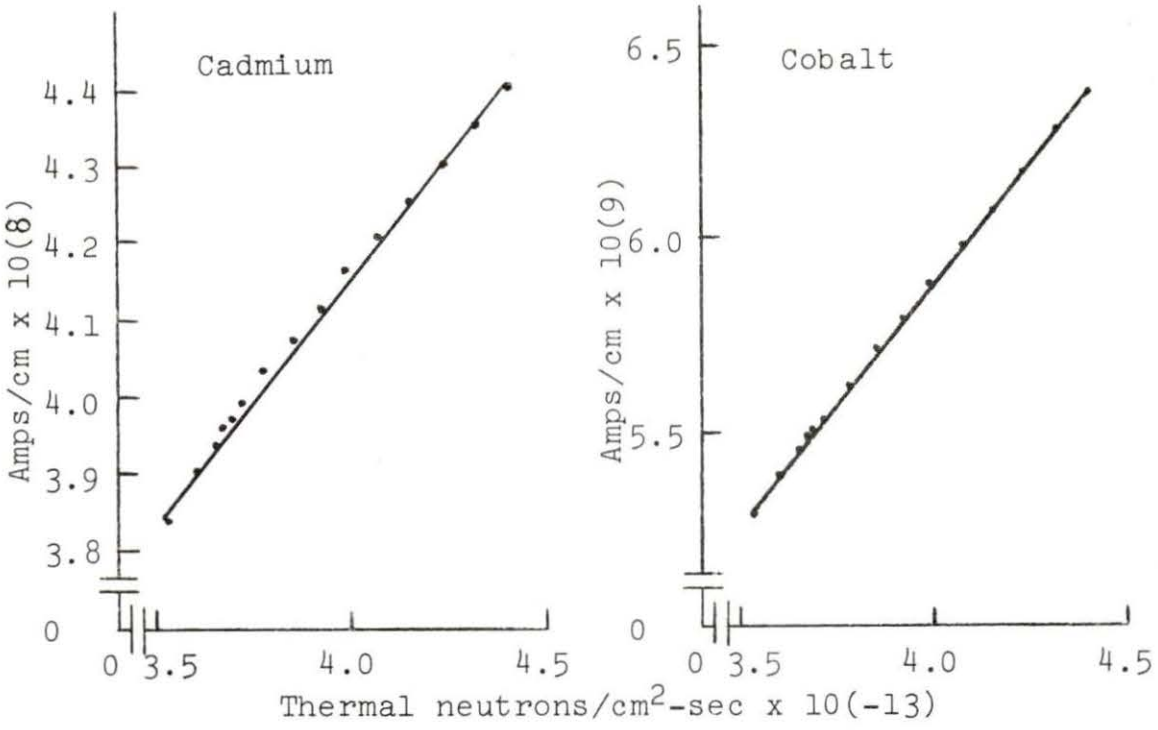

Figure 6.2. Current produced by self-powered neutron detectors versus thermal flux

capture rate of the emitter, and the neutron capture rate is, of course, directly dependent on the flux. The thermal neutron capture rate of the emitter materials used is much higher than that for neutrons of higher energies because their thermal cross sections are much larger than their higher energy cross sections (See Table 5.5). Therefore, the detectors should be highly dependent on the thermal neutron flux.

B. Conclusions

This investigation has shown that the output current developed by a self-powered neutron detector using either Cobalt or Cadmium as an emitter will decrease as the void fraction increases in a typical BWR. The results also show that this current response is almost linear for void fractions less than 0.90. It was observed that the detector response using either of these two emitter materials is directly proportional to the thermal flux corresponding to void fraction changes.

VII. SUGGESTIONS FOR FURTHER RESEARCH

The following are suggestions for further investigation related to this work:

1) The same study should be carried out using transport theory rather than diffusion theory in order to extend the range of validity of the results. Transport theory would make it possible to study in detail the effects on the neutron flux of void fractions close to unity which diffusion theory has difficulty in representing.

2) A dynamic model for the void fraction fluctuations should be developed, and the dynamic response of self-powered detectors determined using the approach developed in this work.

3) The effects of core geometry changes on the relationship of neutron flux to void fraction could be examined. That is, what would be the effect of changing the pitch or lattice geometry on the neutron flux response to a change in void fraction? Such a study would test the general applicability of this analysis of self-powered detector response.

4) Other emitter materials might be examined for their effect on the void thermalization response of a detector.

5) The relative effects on the current output of a self-powered neutron detector of the following phenomena caused by a fluctuating void fraction could be explored: (a) the shift of the neutron spectrum caused by changes in neutron

moderation; and (b) the changes in the number of fissions taking place because of the shifting neutron spectrum.

VIII. LITERATURE CITED

1. Seifritz, W. 1972. An analysis of the space dependent neutron flux density fluctuations at the Lingen Boiling Water Reactor (KWL) by methods of stochastic processes. Atomkernenergie 19: 271-279.

2. Rothmann, George P. 1973. Neutron noise in boiling reactors. Atomkernenergie 21: 113-118.

3. Jaschik, W., and W. Seifritz. 1974. Model for calculating prompt-response self-powered neutron detectors. Nucl. Sci. Engr. 53: 61-72.

4. Stegemann, D., P. Gebureck, A. T. Nikulski, and W. Seifritz. 1973. Operating characteristics of a boiling water reactor deduced from in-core measurements. Pages 15-1 - 15-17 in T. W. Kerlin, ed. Power Plant Dynamics, Control and Testing and Applications Symposium. University of Tennessee, Knoxville, Tennessee.

5. Gebureck, P., W. Hofmann, W. Jaschik, W. Seifritz, and D. Stegemann. 1973. Development and in-core application of self-powered neutron detectors. Paper IAEA-SM-168/G-8. IAEA - Symposium on Nuclear Power Plant Control and Instrumentation, Prague.

6. Wach, D., and G. Kosaly. 1974. Investigation of the joint effect of local and global driving sources in incore-neutron noise measurements. Atomkernenergie 23: 244-250.

7. Kosaly, G., L. Maroti, and L. Mesko. 1974. A simple space dependent theory of the neutron noise in a boiling water reactor. (Paper presented at the Specialists Meeting on Reactor Noise, Rome, Italy, October, 1974.)

8. Lahey, R. T., Jr. 1974. Two-phase flow in boiling water nuclear reactors. NEDO-13388. (General Electric Boiling Water Reactor Systems Department, San Jose, Cal.) 108pp.

9. Paustian, Harold, H. 1975. Effect of steam voids on in-core detector response in boiling water reactors. M. S. Thesis. Iowa State University, Ames, Ia. 93 pp.

10. Barry, R. F. 1963. LEOPARD, a spectrum dependent non-spatial depletion code for the IBM-7094. WCAP-3269-26. (Westinghouse Atomic Power Division, Pittsburgh, Pa.) 65 pp.

11. Strawbridge, L. E. 1963. Calculation of lattice parameters and criticality for uniform water moderated lattices. WCAP-3269-25. (Westinghouse Atomic Power Division, Pittsburgh, Pa.) 33 pp.

12. Crudele, Joseph Samuel. 1973. Study of Ames Laboratory Research Reactor physics characteristics by few group design techniques. Ph.D. Thesis. Iowa State University, Ames, Ia. 119 pp.

13. Flatt, H. P. 1961. The FOG one-dimensional neutron diffusion equation codes. NAA-SR-6104. (Atomics International, Canoga Park, Cal.) 47 pp.

14. Munson, Steven T. 1973. The FOG code. M. E. Paper. Iowa State University, Ames, Ia. 63 pp.

15. McElroy, W. N., R. G. Hawkins, and S. Berg. 1967. A computer-automated iterative method for neutron flux spectra determination by foil activation. AFWL-TR-67-41 Vol. III. (Atomics International, Canoga Park, Cal.)

IX. ACKNOWLEDGMENTS

The author gratefully acknowledges the assistance of the Department of Chemical Engineering and Nuclear Engineering in providing funds for computer operation. In addition, the author wishes to express special appreciation to his major professor, Dr. Donald M. Roberts, for his helpful discussions and suggestions, and to Dr. A. F. Rohach for his help with the computer programs.

X. APPENDIX: DESCRIPTION OF THE SPOND PROGRAM

A. Introduction

SPOND calculates the current output of a self-powered neutron detector given a four-group neutron flux. Input for the program is not formatted and therefore the flow chart or the program list must be examined to put the data in correctly. Output simply consists of listing the void fraction case, the corresponding current output, and the four-group neutron flux is repeated in the output for convenience. The program also prints out all input information as a check. A flow chart and listing of SPOND follows.

FLOW CHART FOR SPOND[1]

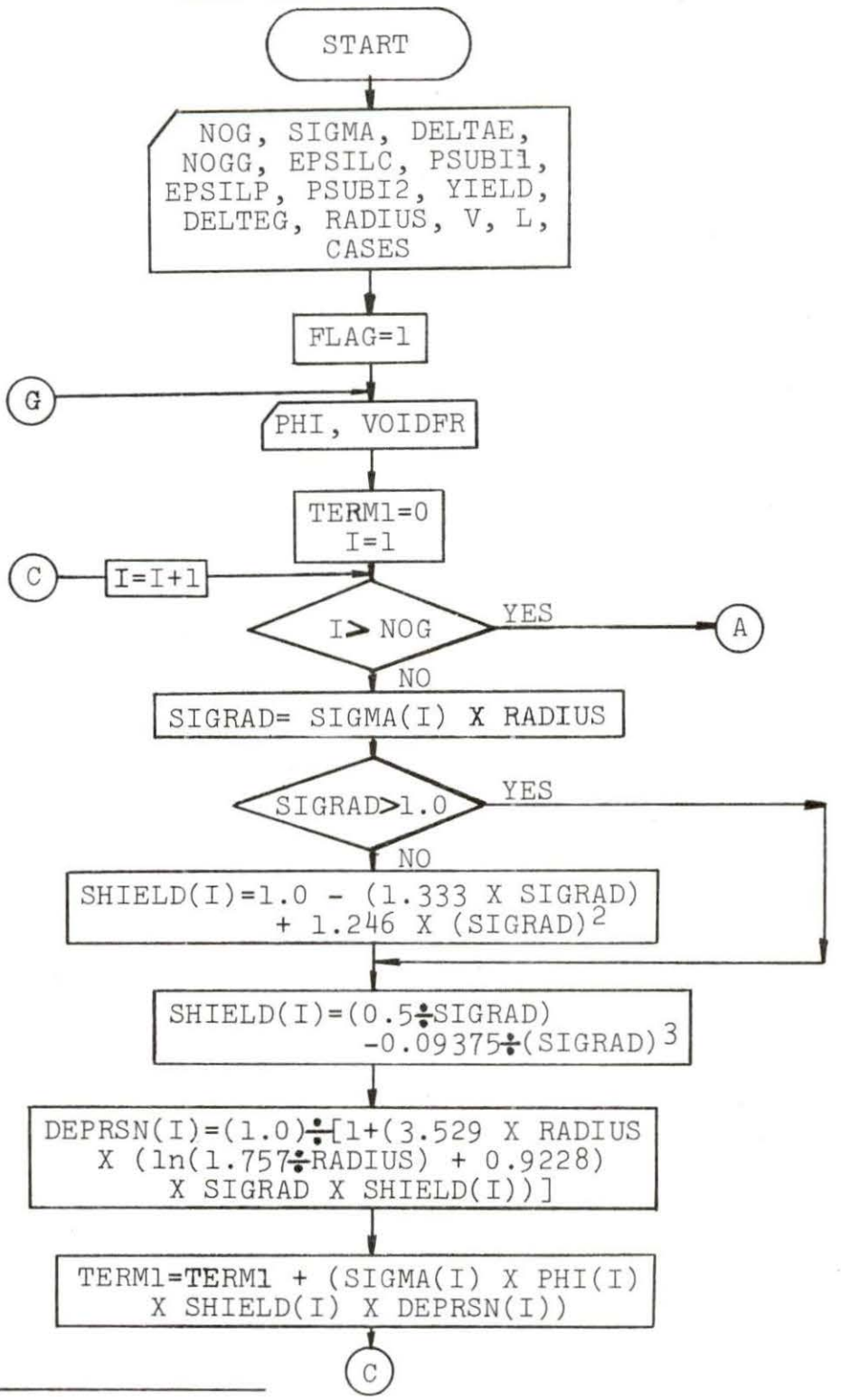

[1] See list of definitions following this section.

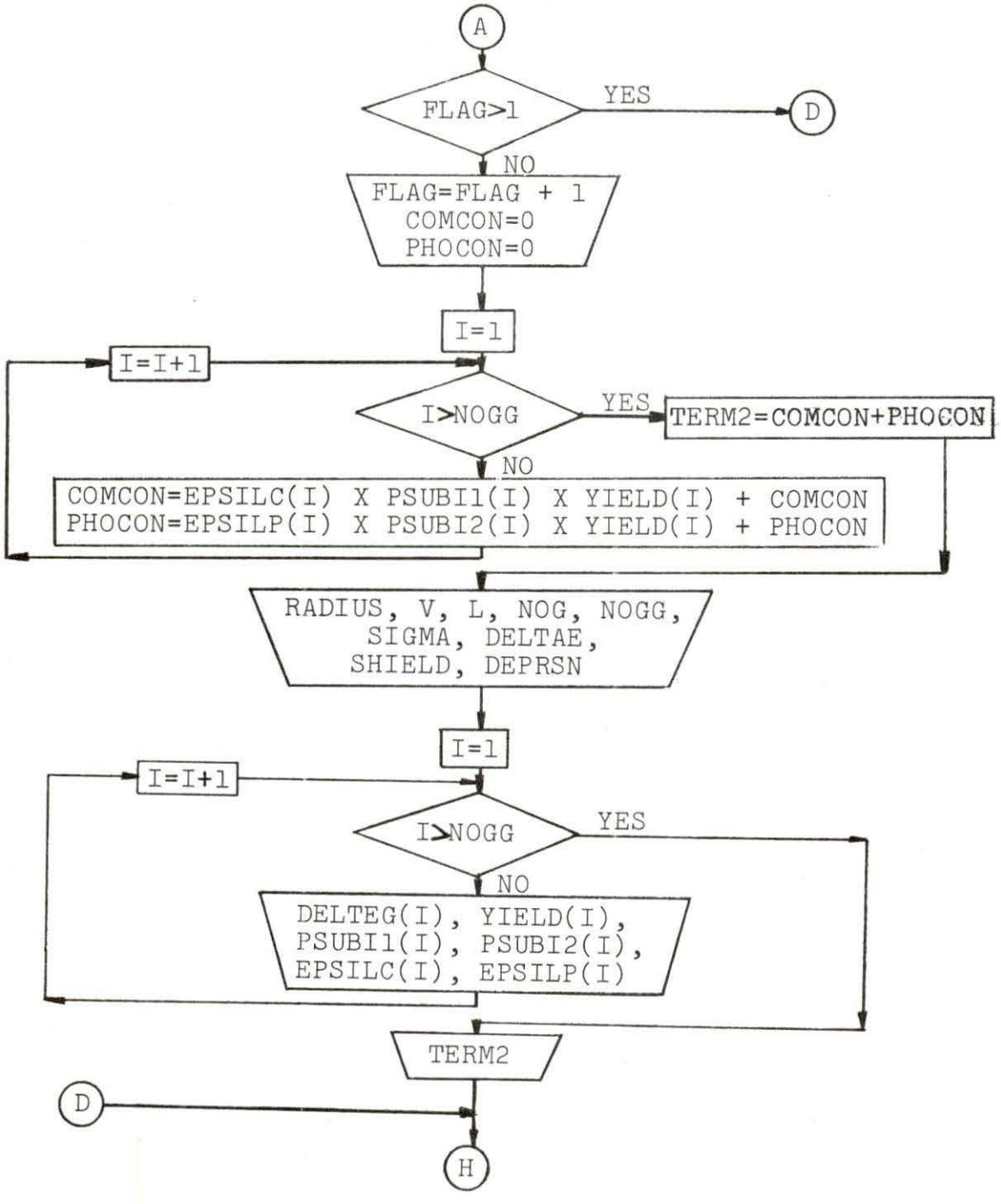
A
FLAG>1
YES
D
NO
FLAG=FLAG + 1
COMCON=0
PHOCON=0
I=1
I=I+1
I>NOGG
YES
TERM2=COMCON+PHOCON
NO
COMCON=EPSILC(I) X PSUBI1(I) X YIELD(I) + COMCON
PHOCON=EPSILP(I) X PSUBI2(I) X YIELD(I) + PHOCON
RADIUS, V, L, NOG, NOGG,
SIGMA, DELTAE,
SHIELD, DEPRSN
I=1
I=I+1
I>NOGG
YES
NO
DELTEG(I), YIELD(I),
PSUBI1(I), PSUBI2(I),
EPSILC(I), EPSILP(I)
TERM2
D
H

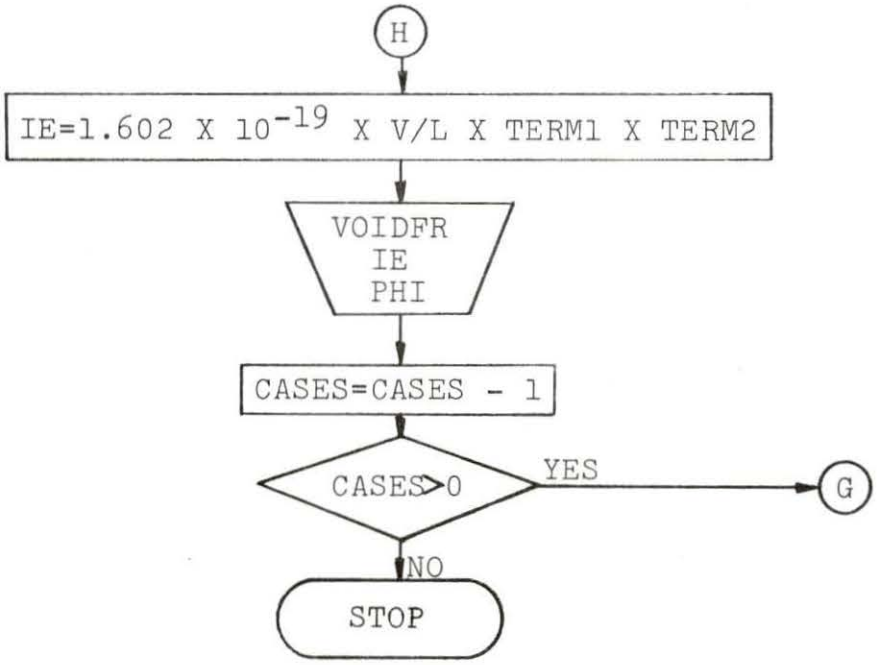
H
IE=1.602 X 10^-19 X V/L X TERM1 X TERM2
VOIDFR
IE
PHI
CASES=CASES - 1
CASES>0
YES
G
NO
STOP

B. SPOND Variable List

NOG = number of neutron energy groups

SIGMA = absorption cross section data for emitter, entered by highest energy group down to lowest

DELTAE = neutron energy group intervals, beginning with highest

NOGG = number of gamma energy groups

EPSILC = electron escape efficiency of Compton electrons, beginning with lowest gamma energy group

PSUBI1 = probability of electron production by Compton effect of a gamma ray, beginning with lowest energy group

EPSILP = electron escape efficiency of photoelectrons, beginning with lowest gamma energy group

PSUBI2 = probability of electron production by photon interaction, beginning with lowest energy

YIELD = the number of gamma rays produced per gamma energy interval per neutron captured in emitter, entered beginning with lowest gamma energy group

DELTEG = gamma energy group intervals, beginning with lowest

RADIUS = radius of emitter

V = volume of emitter

L = length of emitter

CASES = number of void fraction cases being run

PHI = neutron group flux values, entered beginning with

highest neutron energy group

VOIDFR = void fraction associated with the particular flux values being entered

C. SPOND Program List

```
 1          REAL TERM1, SIGRAD, SIGMA(4), RADIUS, SHIELD(4), PHI(4),
           CDEPRSN(4), DELTAE(4), COMCON, PHOCON, EPSILC(30), PSUBI1(30),
           CYIELD(30), DELTEG(30), EPSILP(30), PSUBI2(30), TERM2, IE, V, L,
           CVOIDFR, CASES
 2          INTEGER NOG, NOGG, FLAG
 3          READ, NOG, SIGMA, DELTAE
 4          READ, NOGG, EPSILC, PSUBI1, EPSILP, PSUBI2, YIELD, DELTEG
 5          READ, RADIUS, V, L
 6          READ, CASES
 7          FLAG=1
 8       90 CONTINUE
 9          READ, PHI, VOIDFR
10          TERM1=0.0
11          DO 10 I=1, NOG
12          SIGRAD=SIGMA(I)*RADIUS
13          IF (SIGRAD.GT.1.0) GO TO 5
14          SHIELD(I)=1.0-(1.333*SIGRAD)+(1.246*(SIGRAD**2))
15          GO TO 6
16        5 CONTINUE
17          SHIELD(I)=(0.5/SIGRAD)-(0.09375/(SIGRAD**3))
18        6 CONTINUE
19          DEPRSN(I)=1.0/(1.0+((3.529*RADIUS)*(ALOG(1.757/RADIUS)+0.9228)*SIG
           CRAD*SHIELD(I)))
20          TERM1=TERM1+SIGMA(I)*PHI(I)*SHIELD(I)*DEPRSN(I)
21       10 CONTINUE
22          IF (FLAG.GT.1)GO TO 80
23          FLAG=FLAG+1
24          COMCON=0.0
25          PHOCON=0.0
26          DO 20 I=1, NOGG
27          COMCON=EPSILC(I)*PSUBI1(I)*YIELD(I)+COMCON
28          PHOCON=EPSILP(I)*PSUBI2(I)*YIELD(I)+PHOCON
29       20 CONTINUE
```

```
30          TERM2=COMCON+PHOCON
31          PRINT, RADIUS, V, L
32          PRINT, NOG, NOGG
33          PRINT, SIGMA, DELTAE
34          PRINT, SHIELD, DEPRSN
35          DO 77 I=1, NOGG
36          PRINT70, DELTEG(I), YIELD(I), PSUBI1(I), PSUBI2(I), EPSILC(I), EPS
          CILP(I)
37        70 FORMAT (' ',6F12.6)
38        77 CONTINUE
39          PRINT, TERM2
40          PRINT30
41        30 FORMAT('1','DETECTOR CURRENT OUTPUT PER UNIT LENGTH VS. VOID FRACT
          CION')
42          PRINT 40
43        40 FORMAT ('0','VOID FRACTION',5X,'CURRENT',5X,'GROUP 1 FLUX',3X,'GRO
          CUP 2 FLUX',3X,'GROUP 3 FLUX',3X,'GROUP 4 FLUX')
44        80 CONTINUE
45          IE=1.602E-19*V/L*TERM1*TERM2
46          PRINT50, VOIDFR, IE, PHI
47        50 FORMAT (' ',E11.4,5E15.4)
48          CASES=CASES-1.0
49          IF (CASES.GT.0.0) GO TO 90
50          PRINT 55
51        55 FORMAT ('1','RUN INFORMATION')
52          STOP
53          END
```